Int J Adv Manuf Technol (2002) 19:174–179

The International Journal of
Advanced
Manufacturing
Technology

Error Analysis of a Serial–Parallel Type Machine Tool

J.-W. Zhao[2], K.-C. Fan[1], T.-H. Chang[3] and Z. Li[2]

[1]Department of Mechanical Engineering, National Taiwan University, Taiwan; [2]School of Mechanical Engineering, Huazhong University of Science and Technology, Wuhan, China; and [3]Mechanical Industry Research Lab, ITRI, Taiwan

In order to evaluate the accuracy of a serial–parallel type machine tool, an error analysis is presented. Two different methods are adopted to derive the error model, namely the linkage kinematic analysis and the differential vector method, by which the effects of strut manufacturing tolerance and actuating error on the tool position and pose are investigated. The computational results show the influences of the actuating error and the strut length error on the machine tool inaccuracies.

Keywords: Accuracy evaluation; Error analysis; Error modelling; Kinematic analysis; Manufacturing tolerance; Serial–parallel machine tool

1. Introduction

To obtain higher accuracy and greater dexterity, machine tool manufacturers are developing parallel structures for the next generation of machine tools. It is always a goal to pursue an interesting development in the machine tool industry that holds great promise for improving accuracy. Based on a three-degrees-of-freedom parallel shaft platform, a new five-degrees-of-freedom CNC machining structure has been developed. It is believed that a machine tool of a parallel structure will be enhanced in rigidity compared to a conventional multi-axis structure, as discussed by Lee et al. [1], and Lebret et al. [2].

Many publications dealing with the kinematics of Steward platform-based manipulators have appeared in recent years, such as [3–5]. Most of these papers have focused on discussing both analytical and numerical methods to solve the forward kinematics of pure-parallel mechanisms, as discussed in [6–8]. Several papers discussed the accuracy analysis of a parallel manipulator. Wang and Masory [9] investigated how manufacturing errors affect the accuracy of a Steward platform. Ropponen and Arai [10] and Patel and Ehmann [11] presented an error model based on the differential leg length of a Steward platform. However, very few publications have dealt with the verification of error modelling methods for parallel machine tool structures.

The machine tool studied is called a serial–parallel machine tool. It consists of serial units (*X–Y* table, column and slider) and a parallel shaft platform. In this study, the error model was derived using two methods, namely linkage kinematic error analysis and the differential vector method. The agreement of final forms is verified. Computational examples indicate some major factors contributing to inaccuracies.

2. Machine Tool Configuration

The structure of the serial–parallel machine tool is shown in Fig. 1. It consists of a three-degrees-of-freedom parallel shaft platform including two angular orientations in pitch (about the *y*-axis) and yaw (about the *x*-axis) and one linear motion in the vertical direction, and a conventional two-degrees-of-

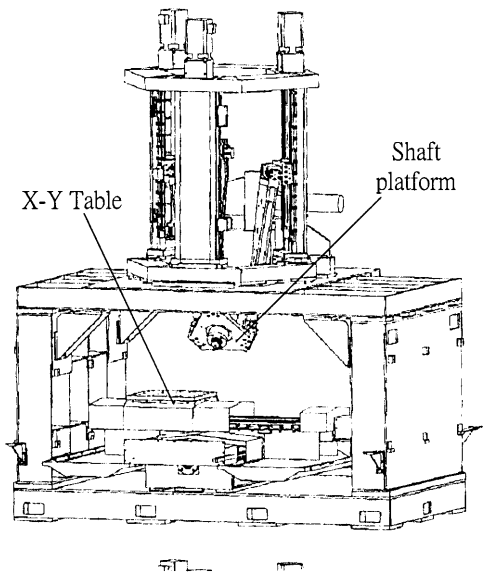

Fig. 1. Machine tool structure.

Correspondence and offprint requests to: Professor Kuang-Chao Fan, Department of Mechanical Engineering, National Taiwan University, Taipei, Taiwan. E-mail: fan@ccms.ntu.edu.tw

freedom *X–Y* table which carries the workpiece and provides motions in two horizontal directions. It is noted here that the rotational motion, either pitch or yaw, is not a pure rotation, but is accompanied by translation with components perpendicular to the named linear degree of freedom. The spindle is assembled in the platform, which is connected to three constant length struts by means of ball joints (or *U*-joints) which are equally spaced at 120°. The other end of each strut is connected to a slider with a rotational joint. Each slider moves up and down along the corresponding columns (vertical slideway) which are also spaced at 120° from one another. The *X–Y* motion is implemented using a standard *X–Y* table and a servo feed device.

3. Nominal Kinematics

To synthesise the kinematics of the machine tool, three relative coordinate frames are shown in Fig. 2. A static Cartesian coordinate frame *XYZ* is fixed at the base of the machine tool with the *Z*-axis pointing in the vertical direction, the *X*-axis points toward A_1, and the *Y*-axis points along the A_2A_3 line. The movable Cartesian coordinate frame, $X'Y'Z'$, is fixed at the centre of the *X–Y* table with the same axes directions as the *XYZ* coordinate frame. The third coordinate frame *xyz* is assigned to the tool tip, with the *z*-axis coinciding with the shaft axis. The ball joint b_1 is located in plane xO_Tz .

Coordinate frame *xyz*, with respect to the coordinate frame *XYZ*, can be described by a homogeneous transformation matrix [*T*] which represents the shaft platform spatial location.

$$[T] = \begin{bmatrix} k_1 & m_1 & n_1 & x_T \\ k_2 & m_2 & n_2 & y_T \\ k_3 & m_3 & n_3 & z_T \\ 0 & 0 & 0 & 1 \end{bmatrix}$$

$$= \begin{bmatrix} \cos\beta\cos\gamma & -\cos\beta\sin\gamma & \sin\beta & x_T \\ \sin\alpha\sin\beta\cos\gamma + \cos\alpha\sin\gamma & -\sin\alpha\sin\beta\sin\gamma + \cos\alpha\cos\gamma & -\sin\alpha\cos\beta & y_T \\ -\cos\alpha\sin\beta\cos\gamma + \sin\alpha\sin\gamma & \cos\alpha\sin\beta\sin\gamma + \sin\alpha\cos\gamma & \cos\alpha\cos\beta & z_T \\ 0 & 0 & 0 & 1 \end{bmatrix} \quad (1)$$

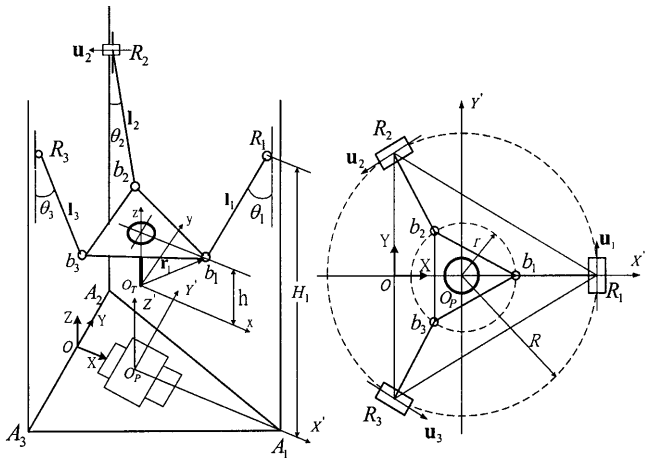

Fig. 2. Schematic diagram of the serial–parallel structure.

where $[x_T\ y_T\ z_T]^T$ is the position vector of the origin of the frame *xyz*, and the orientation unit vectors $\mathbf{k} = [k_1\ k_2\ k_3]^T$, $\mathbf{m} = [m_1\ m_2\ m_3]^T$, and $\mathbf{n} = [n_1\ n_2\ n_3]^T$ are directional cosines of the *x*-, *y*- and *z*-axes with respect to the coordinate frame *XYZ*. α, β, and γ are the Euler angles which specify three successive angular motions of the spindle platform with respect to the *X*-, *Y*-, and *Z*-axes.

Therefore, the Cartesian position of the ball joints $\mathbf{b}_i$ with respect to the coordinate frame *XYZ* can be expressed as

$$\begin{bmatrix} \mathbf{b}_i \\ 1 \end{bmatrix}_o = {}^o_{o_p}[T] \cdot {}^{o_P}_{o_T}[T] \cdot \begin{bmatrix} \mathbf{b}_i \\ 1 \end{bmatrix}_{o_T}$$

$$= [T] \cdot \begin{bmatrix} \mathbf{b}_i \\ 1 \end{bmatrix}_{o_T} \quad (i = 1, 2, 3) \quad (2)$$

From Fig. 2, $\mathbf{b}_i$ in the $(x, y, z)_T$ coordinate system can be expressed in the following vector forms:

$$\mathbf{b}_1 = [r \quad 0 \quad h]^T$$

$$\mathbf{b}_2 = \left[-\frac{r}{2} \quad \frac{\sqrt{3}}{2} r \quad h \right]^T$$

$$\mathbf{b}_3 = \left[-\frac{r}{2} \quad -\frac{\sqrt{3}}{2} r \quad h \right]^T$$

Substituting these vector forms into Eq. (2) yields

$$\begin{bmatrix} \mathbf{b}_1 \\ 1 \end{bmatrix}_o = [T] \cdot \begin{bmatrix} \mathbf{b}_1 \\ 1 \end{bmatrix}_{o_T} = \begin{bmatrix} X_1 \\ Y_1 \\ Z_1 \\ 1 \end{bmatrix} = \begin{bmatrix} rk_1 + hn_1 + x_T \\ rk_2 + hn_2 + y_T \\ rk_3 + hn_3 + z_T \\ 1 \end{bmatrix}$$

$$\begin{bmatrix} \mathbf{b}_2 \\ 1 \end{bmatrix}_o = [T] \cdot \begin{bmatrix} \mathbf{b}_2 \\ 1 \end{bmatrix}_{o_T} = \begin{bmatrix} X_2 \\ Y_2 \\ Z_2 \\ 1 \end{bmatrix} = \begin{bmatrix} -\frac{r}{2}k_1 + \frac{\sqrt{3}r}{2}m_1 + hn_1 + x^T \\ -\frac{r}{2}k_2 + \frac{\sqrt{3}r}{2}m_2 + hn_2 + y_T \\ -\frac{r}{2}k_3 + \frac{\sqrt{3}r}{2}m_3 + hn_3 + z_T \\ 1 \end{bmatrix}$$

$$\begin{bmatrix} \mathbf{b}_3 \\ 1 \end{bmatrix}_o = [T] \cdot \begin{bmatrix} \mathbf{b}_3 \\ 1 \end{bmatrix}_{o_T} = \begin{bmatrix} X_3 \\ Y_3 \\ Z_3 \\ 1 \end{bmatrix} = \begin{bmatrix} -\frac{r}{2}k_1 - \frac{\sqrt{3}r}{2}m_1 + hn_1 + x_T \\ -\frac{r}{2}k_2 - \frac{\sqrt{3}r}{2}m_2 + hn_2 + y_T \\ -\frac{r}{2}k_3 - \frac{\sqrt{3}r}{2}m_3 + hn_3 + z_T \\ 1 \end{bmatrix} \quad (3)$$

As the struts are constrained by the rotational joints (R_1, R_2, R_3), each strut can move only in its respective plane: $Y_1 = 0$, $Y_2 = -\sqrt{3}\,(X_2 - R/2)$, and $Y_3 = \sqrt{3}\,(X_3 - R/2)$. Substituting these three boundary conditions into Eq. (3) the following equations can be derived:

$$\gamma = -\arctan\left(\frac{\sin\alpha\sin\beta}{\cos\alpha + \cos\beta}\right)$$

and

$$x_T = \frac{r}{2}(k_1 - m_2) - hn_1 + \frac{R}{2} = \frac{r}{2}$$
$$(\cos\beta\cos\gamma + \sin\alpha$$
$$\sin\beta\sin\gamma - \cos\alpha\cos\gamma) - h\sin\beta + \frac{R}{2}$$
$$y_T = -(rk_2 + hn_2) = h\sin\alpha\cos\beta \quad (4)$$
$$- r\sin\alpha\sin\beta\cos\gamma - r\cos\alpha\sin\gamma$$

where R and r are the radii of circles passing through joints R_i and b_i ($i = 1, 2, 3$), respectively; h is the distance from the tool tip o_T to the centre of platform.

Equation (3) indicates that γ is dependent on the angles α and β. Equation (4) indicates that x_T and y_T are both functions of directional cosines. In other words, x_T and y_T are dependent only on the shaft platform pose.

From Eqs (3) and (4), if α, β, and z_T are given, the transformation matrix $[T]$ is determined. The spatial position of each ball joint with respect to XYZ can be calculated using Eq. (2). As the strut length is constant, the position component of each slider in the Z-axis can be calculated according to inverse kinematics as

$$H_i = R_{iZ} = \sqrt{(l_i^2 - (R_{iX} - b_{iX})^2 - (R_{iY} - b_{iY})^2)} + b_{iZ} \quad (i = 1, 2, 3) \quad (5)$$

where H_i is the height of joint R_i in the Z-axis; l_i is the strut length.

4. Volumetric Error Analysis

Owing to the inherent machine errors, the tool will inevitably deviate from its nominal position. Some likely error sources that can cause machine tool inaccuracy include: errors in manufacturing and assembly; kinematic errors in the mechanism; control system errors; elastic deformation; and thermal deformation.

To assess the machine tool volumetric accuracy, it is necessary to model the position and orientation error equations for the shaft platform. Two methods for error modelling are proposed to verify the displacement and orientation errors as described below.

4.1. Error Modelling Using Linkage Kinematic Analysis

Many factors can be attributed to shaft platform errors. If the position and pose errors of the tool tip are caused only by linear servo feed device and strut length errors, the derivation steps for the error model using linkage kinematics are as follows.

The tool tip (origin of the platform coordinate frame xyz) position error vector $\mathbf{e}$ and platform orientation error vector $\boldsymbol{\epsilon}$ with respect to frame XYZ can be defined as

$$\mathbf{e} = [e_x\ e_y\ e_z]^T$$
$$\boldsymbol{\epsilon} = [\epsilon_x\ \epsilon_y\ \epsilon_z]^T \quad (6)$$

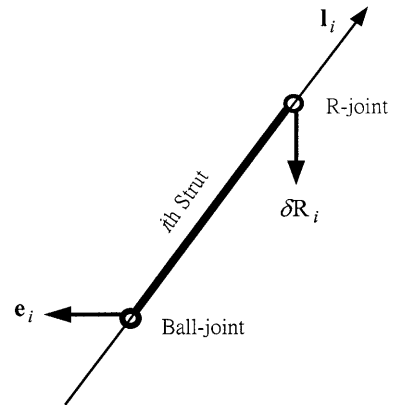

Fig. 3. Diagram of the joint position error vectors.

The position error vector $\mathbf{e}_i$ of ball joint b_i can be obtained by

$$\mathbf{e}_i = \mathbf{e} + \boldsymbol{\epsilon} \times \mathbf{r}_i \quad (7)$$

where $\mathbf{r}_i$ denotes the vector from the tool tip to each ball joint with respect to the frame XYZ.

The rigid strut is assumed to be in a kinematic state. The projection of $\mathbf{e}_i$ to $\mathbf{l}_i$ is equal to the projection of $\delta\mathbf{R}_i$ to $\mathbf{l}_i$, plus the strut length error δl_i (see Fig. 3). That is to say, the position errors of the ball joints are caused by the position errors of rotation joints and the strut length error.

$$\mathbf{e}_i \cdot \mathbf{l}_i = \delta\mathbf{R}_i \cdot \mathbf{l}_i + \delta l_i \quad (i = 1, 2, 3) \quad (8)$$

where,

$\mathbf{l}_i = \frac{1}{l_i}(\mathbf{R}_i - \mathbf{b}_i)$ is a directional unit vector for each strut

$\delta\mathbf{R}_i$ is the rotation joint position error vector with respect to the frame XYZ

δl_i is the strut length error

Inserting Eq. (7) into Eq. (8) yields

$$\mathbf{l}_i \cdot \mathbf{e} + (\mathbf{r}_i \times \mathbf{l}_i) \cdot \boldsymbol{\epsilon} = \mathbf{l}_i \cdot \delta\mathbf{R}_i + \delta l_i \quad (i = 1, 2, 3) \quad (9)$$

Presenting Eq. (9) in matrix form gives:

$$[\mathbf{l}]\ \mathbf{e} + [\mathbf{l}_o]\ \boldsymbol{\epsilon} = [\mathbf{l}']\ \delta\mathbf{R} + \delta\mathbf{l} \quad (10)$$

where,

$$[\mathbf{l}] = [\mathbf{l}_1^T\ \mathbf{l}_2^T\ \mathbf{l}_3^T]^T = \begin{bmatrix} l_{1x} & l_{1y} & l_{1z} \\ l_{2x} & l_{2y} & l_{2z} \\ l_{3x} & l_{3y} & l_{3z} \end{bmatrix} \in R^{3\times3}$$

$$[\mathbf{l}_0] = \begin{bmatrix} (\mathbf{r}_1 \times \mathbf{l}_1)^T \\ (\mathbf{r}_2 \times \mathbf{l}_2)^T \\ (\mathbf{r}_3 \times \mathbf{l}_3)^T \end{bmatrix} = \begin{bmatrix} (\mathbf{r}_1 \times \mathbf{l}_1)_x & (\mathbf{r}_1 \times \mathbf{l}_1)_y & (\mathbf{r}_1 \times \mathbf{l}_1)_z \\ (\mathbf{r}_2 \times \mathbf{l}_2)_x & (\mathbf{r}_2 \times \mathbf{l}_2)_y & (\mathbf{r}_2 \times \mathbf{l}_2)_z \\ (\mathbf{r}_3 \times \mathbf{l}_3)_x & (\mathbf{r}_3 \times \mathbf{l}_3)_y & (\mathbf{r}_3 \times \mathbf{l}_3)_z \end{bmatrix} \in R^{3\times3}$$

$$[\mathbf{l}'] = \begin{bmatrix} \mathbf{l}_1^T & \Lambda & 0 & 0 & 0 \\ M & & \mathbf{l}_2^T & & M \\ 0 & 0 & 0 & \Lambda & \mathbf{l}_3^T \end{bmatrix} \in R^{3\times9}$$

$$\delta\mathbf{R} = [\delta\mathbf{R}_1\ \delta\mathbf{R}_2\ \delta\mathbf{R}_3]^T \in R^{9\times 1}$$

$$\delta\mathbf{l} = [\delta l_1\ \delta l_2\ \delta l_3]^T \in R^{3\times 1}$$

4.2 Constraint Equations

Equation (10) involves only three simultaneous equations, but there are six elements in total in $\mathbf{e}$ and $\boldsymbol{\epsilon}$. The constraint equations must be derived in order to compute all of the error elements.

Since the strut rotates around the *R*-joint rotation axis, the directional vector of each strut is orthogonal to the axis of the corresponding rotation joint. If $\mathbf{u}_i$ represents the directional unit vector of the joint rotation axis (see Fig. 2), according to Eq. (7) the projection of the ball joint position error onto $\mathbf{u}_i$ is then

$$\mathbf{u}_i \cdot \mathbf{e} + (\mathbf{r}_i \times \mathbf{u}_i) \cdot \boldsymbol{\epsilon} = 0 \quad (i = 1, 2, 3)$$

Expressed in matrix form this yields

$$[\mathbf{u}]\ \mathbf{e} + [\mathbf{u}_o]\ \boldsymbol{\epsilon} = \mathbf{0} \tag{11}$$

where,

$$[\mathbf{u}] = [\mathbf{u}_1^T\ \mathbf{u}_2^T\ \mathbf{u}_3^T]^T = \begin{bmatrix} 0 & 1 & 0 \\ -\frac{\sqrt{3}}{2} & -\frac{1}{2} & 0 \\ \frac{\sqrt{3}}{2} & -\frac{1}{2} & 0 \end{bmatrix} \in R^{3\times 3}$$

$$[\mathbf{u}_0] = [(\mathbf{r}_1 \times \mathbf{u}_1)^T\ (\mathbf{r}_2 \times \mathbf{u}_2)^T\ (\mathbf{r}_3 \times \mathbf{u}_3)^T]^T \in R^{3\times 3}$$

Combining Eqs (10) and (11) yields

$$[\mathbf{J}]\ [\boldsymbol{\Delta}] = [\mathbf{M}]\ [\delta\mathbf{A}] \tag{12}$$

where,

$$[\mathbf{J}] = \begin{bmatrix} [\mathbf{l}] & \mathrm{M} & [\mathbf{l}_0] \\ \Lambda & \Lambda & \Lambda \\ [\mathbf{u}] & \mathrm{M} & [\mathbf{u}_0] \end{bmatrix} \in R^{6\times 6}$$

$$[\boldsymbol{\Delta}] = \begin{bmatrix} \mathbf{e} \\ \boldsymbol{\epsilon} \end{bmatrix} = [e_x\ e_y\ e_z\ \epsilon_x\ \epsilon_y\ \epsilon_z]^T \in R^{6\times 1}$$

$$[\mathbf{M}] = \begin{bmatrix} \mathbf{l}_1^T & & 1 & \Lambda & \Lambda & \Lambda & 0 \\ \mathrm{M} & & \mathrm{M} & \mathbf{l}_2^T & 1 & & \mathrm{M} \\ \mathrm{M} & & \mathrm{M} & & & \mathbf{l}_3^T & 1 \\ \mathrm{M} & & \mathrm{M} & & & & \mathrm{M} \\ \mathrm{M} & & \mathrm{M} & & & & \mathrm{M} \\ 0 & 0 & 0 & 0 & \Lambda & \Lambda & \Lambda & 0 \end{bmatrix} \in R^{6\times 12}$$

$$[\delta\mathbf{A}] = [\delta\mathbf{R}_1\ \delta l_1\ \delta\mathbf{R}_2\ \delta l_2\ \delta\mathbf{R}_3\ \delta l_3]^T \in R^{12\times 1}$$

Equation (12) can be expressed in another form as

$$[\boldsymbol{\Delta}] = [\mathbf{J}]^{-1}\ [\mathbf{M}]\ [\delta\mathbf{A}] \tag{13}$$

where $[\mathbf{J}]^{-1}$ is defined as the inverse of the Jacobian, also called the error transmission matrix.

4.3 Error Modelling Using the Differential Vector Method

It is worth looking at how all the factors affect the machine tool accuracy. In other words, it is necessary to determine the relationship between the error sources and tool tip volumetric errors and platform pose. The differential vector error model can be derived directly from the kinematic vector loop.

The serial–parallel structure with the configuration shown in Fig. 1 consists of three parallel structural loops. Each loop can be identified from the tool tip via the *X–Y* table, column, slider, strut, shaft platform, and back to the tool tip. In each loop, only the errors that act on the cutting tool and workpiece are of importance. A closed vector chain can be drawn, as shown in Fig. 4, and the relations between all vectors are presented in the following equation.

$$\mathbf{C}_i + \mathbf{R}_i + \mathbf{L}_i = \mathbf{O}_P + \mathbf{O}_T + \mathbf{q}_i \quad (i = 1, 2, 3) \tag{14}$$

where,

$\mathbf{C}_i$ is the position vector of the *i*th slider with respect to the origin *O*

$\mathbf{R}_i$ is the vector from the centre of the *i*th slider to the joint R_i

$\mathbf{L}_i$ is the vector from the rotation joint R_i to the ball joint b_i

$\mathbf{O}_P$ is the position vector of *X–Y* table

$\mathbf{O}_T$ is the vector from the tool tip to the center of *X–Y* table

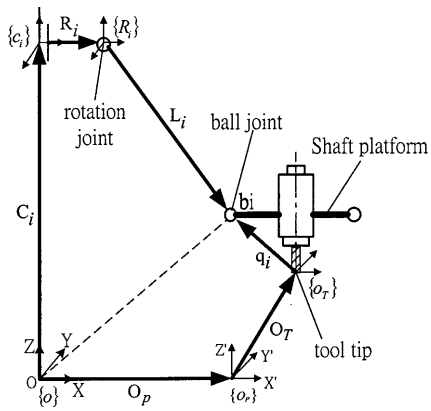

Fig. 4. Vector chain to illustrate relative position.

$\mathbf{q}_i$ is the vector from the tool tip to the ith ball joint

Note that the vectors are all with respect to the coordinate frame XYZ. Therefore, Eq. (14) can also be expressed as

$$\mathbf{C}_i + \mathbf{R}_i + l_i\mathbf{l}_i = \mathbf{O}_P + \mathbf{O}_T + {}^{o}_{o_T}[T]\,{}^{o_T}\mathbf{r}_i \quad (i = 1, 2, 3) \tag{15}$$

where a vector referenced to the coordinate frame $\{o_T\}$ is denoted by ${}^{o_T}\mathbf{r}_i$, and the transformation matrix of the frame $\{o_T\}$ with respect to $\{o\}$ is indicated by ${}^{o}_{o_T}[T]$.

Differentiating Eq. (15) yields

$$\begin{aligned}&\delta\mathbf{C}_i + \delta\mathbf{R}_i + \delta l_i\mathbf{l}_i + l_i\delta\mathbf{l}_i\\ &= \delta\mathbf{O}_P + \delta\mathbf{O}_T + {}^{o}_{o_T}\delta[T]\,{}^{o_T}\mathbf{r}_i + {}^{o}_{o_T}[T]\,{}^{o_T}\delta\mathbf{r}_i\end{aligned} \tag{16}$$

where $\delta\mathbf{O}_T = \mathbf{e} = [e_x\ e_y\ e_z]^T$, and the rotation error matrix is

$${}^{o}_{o_T}\delta[T] = \begin{bmatrix} 0 & -\epsilon_z & \epsilon_y \\ \epsilon_z & 0 & -\epsilon_x \\ -\epsilon_y & \epsilon_x & 0 \end{bmatrix} {}^{o}_{o_T}[T]$$

Thus,

$${}^{o}_{o_T}\delta[T]\,{}^{o_T}\mathbf{r}_i = \boldsymbol{\epsilon} \times \mathbf{r}_i, \quad \boldsymbol{\epsilon} = [\epsilon_x\ \epsilon_y\ \epsilon_z]^T$$

Since $\mathbf{l}_i$ is a directional unit vector, so that from vector operation $\mathbf{l}_i^T\cdot\mathbf{l}_i = 1$ and $\mathbf{l}_i^T\cdot\delta\mathbf{l}_i = 0$. Multiplying Eq. (16) by $\mathbf{l}_i^T$ yields

$$\begin{aligned}&\mathbf{l}_i^T\cdot\mathbf{e} + (\mathbf{r}_i\times\mathbf{l}_i)^T\cdot\boldsymbol{\epsilon} = (\mathbf{l}_i^T\,\delta\mathbf{R}_i + \delta l_i)\\ &+ (\mathbf{l}_i^T\,\delta\mathbf{C}_i - \mathbf{l}_i^T\,{}^{o}_{o_T}[T]\,{}^{o_T}\delta\mathbf{r}_i - \mathbf{l}_i^T\,\delta\mathbf{O}_P) \quad (i = 1, 2, 3)\end{aligned} \tag{17}$$

Applying the same constraint equations, as given by Eq. (11), to Eq. (17) and rearranging into the matrix form yields

$$[\mathbf{J}]\,[\boldsymbol{\Delta}] = [\mathbf{M}]\,[\delta\mathbf{A}] + [\mathbf{N}]\,[\delta\mathbf{B}] \tag{18}$$

where,

$$[\mathbf{J}] = \begin{bmatrix} \mathbf{l}_1^T & (\mathbf{r}_1\times\mathbf{l}_1)^T \\ \mathbf{l}_2^T & (\mathbf{r}_2\times\mathbf{l}_2)^T \\ \mathbf{l}_3^T & (\mathbf{r}_3\times\mathbf{l}_3)^T \\ \mathbf{u}_1^T & (\mathbf{r}_1\times\mathbf{u}_1)^T \\ \mathbf{u}_2^T & (\mathbf{r}_2\times\mathbf{u}_2)^T \\ \mathbf{u}_3^T & (\mathbf{r}_3\times\mathbf{u}_3)^T \end{bmatrix} \in R^{6\times6}$$

$$[\boldsymbol{\Delta}] = \begin{bmatrix} \mathbf{e} \\ \boldsymbol{\epsilon} \end{bmatrix} = [e_x\ e_y\ e_z\ \epsilon_x\ \epsilon_y\ \epsilon_z]^T \in R^{6\times1}$$

$$[\mathbf{M}] = \begin{bmatrix} \mathbf{l}_1^T & & 1 & \Lambda & \Lambda & \Lambda & 0 \\ M & & M & \mathbf{l}_2^T & 1 & & M \\ M & & M & & & \mathbf{l}_3^T & 1 \\ M & & M & & & & M \\ M & & M & & & & M \\ 0 & 0 & 0 & 0 & \Lambda & \Lambda & \Lambda & 0 \end{bmatrix} \in R^{6\times12}$$

$$[\delta\mathbf{A}] = [\delta\mathbf{R}_1\ \delta l_1\ \delta\mathbf{R}_2\ \delta l_2\ \delta\mathbf{R}_3\ \delta l_3]^T \in R^{12\times1}$$

$$[\mathbf{N}] = \begin{bmatrix} \mathbf{l}_1^T & -\mathbf{l}_1^T\,{}^{o}_{o_P}[T] & -\mathbf{l}_1^T & \Lambda & \Lambda & \Lambda & \Lambda & \Lambda & \mathbf{0} \\ M & M & M & \mathbf{l}_2^T & -\mathbf{l}_2^T\,{}^{o}_{o_P}[T] & -\mathbf{l}_2^T & & & M \\ M & M & M & & & & \mathbf{l}_3^T & -\mathbf{l}_3^T\,{}^{o}_{o_P}[T] & -\mathbf{l}_3^T \\ M & M & M & & & & & & M \\ M & M & M & & & & & & M \\ 0 & 0 & 0 & \Lambda & \Lambda & \Lambda & \Lambda & \Lambda & 0 \end{bmatrix} \in R^{6\times27}$$

$$[\delta\mathbf{B}] = [\delta\mathbf{C}_1\ {}^{o_T}\delta\mathbf{r}_1\ \delta\mathbf{O}_P\ \Lambda\ \Lambda\ \delta\mathbf{C}_3\ {}^{o_T}\delta\mathbf{r}_3\ \delta\mathbf{O}_3]^T \in R^{27\times1}$$

Alternatively, Eq. (18) can be presented in the following form

$$[\boldsymbol{\Delta}] = [\mathbf{J}]^{-1}\,[\mathbf{M}]\,[\delta\mathbf{A}] + [\mathbf{J}]^{-1}\,[\mathbf{N}]\,[\delta\mathbf{B}] \tag{19}$$

The error sources considered in this model are combined in the matrices [**M**] and [**N**], including manufacturing error, assembly error, and actuating error etc.

4.4 Comparisons

It is apparent that if error items δC_i, ${}^{o_T}\delta\mathrm{r}_i$, and δO_P are ignored, namely the matrix $[\delta\mathbf{B}] = 0$, Eq. (19) will be in the same form as Eq. (13). The difference in the error models derived using the two different approaches depends only on the error factors to be considered. The consistency of the error model used to analyse this machine tool accuracy has, therefore, been verified.

5. Simulation Examples

In order to study the tool tip position errors and the platform orientation errors, a simulation example was performed using the following nominal parameters:

$$\dot{R} = 400 \text{ mm}$$

$$r = 200 \text{ mm}$$

$$h = 300 \text{ mm}$$

$$l_1 = l_2 = l_3 = 1000 \text{ mm}$$

Assuming that a certain error occurred in the strut length δl_i and the platform rotation angles α and β referenced to the coordinate frame XYZ of: $|\delta l_i| = 0.06$ mm (around accuracy grade IT6), $\alpha = 15°$, $\beta = 10°$, and $z_T = 300$ mm, the error transformation matrix $[\mathbf{J}]^{-1}$, matrix [**M**] and [**N**] can then be constructed using Eqs (1) to (4).

The position and orientation errors were computed using the different magnitude of $\|\delta\mathbf{R}_i\|$, while the platform pose was kept unchanged. The resultant tool tip position errors and platform orientation errors are given, respectively, in Figs 5(a) and 5(b), in which $\delta\mathbf{R}_i$ (i = 1, 2, 3) has the same norm to affect the shaft platform. Figure 6 shows the error graphs in which only $\delta\mathbf{R}_1$ is effective. Similarly, the error diagrams can also be computed with either $\delta\mathbf{R}_2$ or $\delta\mathbf{R}_3$ considered individually.

From Fig. 5, it can be seen that the tool tip vertical positioning error e_z is influenced significantly when all sliding errors are of the same amount. In such a condition, horizontal

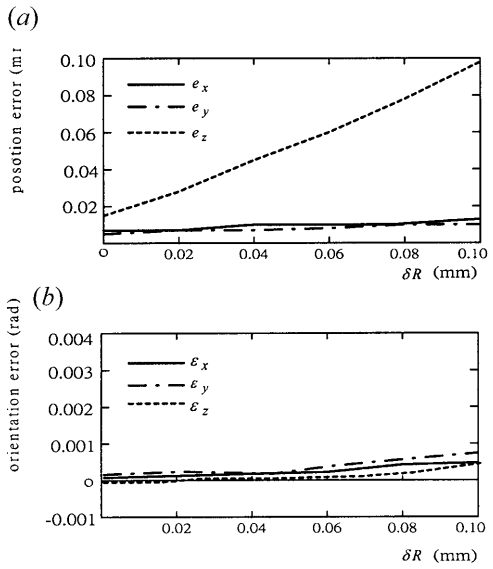

Fig. 5. Tool tip (*a*) position error and (*b*) pose error. ($\|\delta\mathbf{R}_1\| = \|\delta\mathbf{R}_2\| = \|\delta\mathbf{R}_3\| = \delta R$, $\alpha = 15°$, $\beta = 10°$).

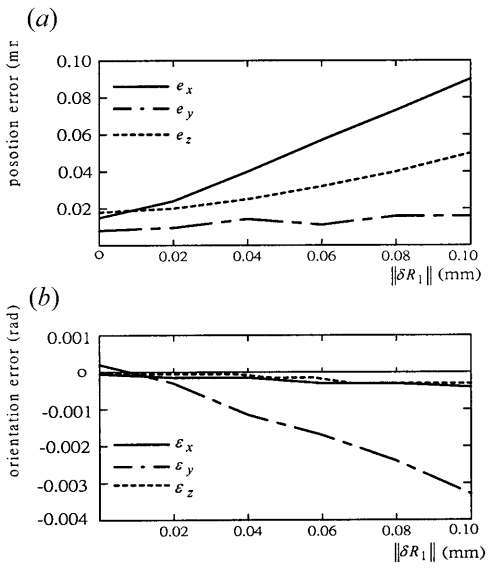

Fig. 6. Tool tip (*a*) position error and (*b*) pose error. ($\|\delta\mathbf{R}_1\|$ only, $\alpha = 15°$, $\beta = 10°$).

position errors e_x and e_y, and all orientation errors ϵ_x, ϵ_y, and ϵ_z are less significant because of the geometric symmetry. It can also be found that if only one sliding error is effective, corresponding position errors and rotation errors will be caused, as shown in Fig. 6.

6. Conclusions

This paper presents the volumetric error analysis for a serial–parallel type machine tool. The error model is derived using two methods. One method uses the accumulated linkage kinematic errors and the other uses the differentiation of the closed vector loop. It has been proved that both methods are consistent in the final form. The error model will be used for analysing the influences of other error sources on the machine tool inaccuracies. From the computational examples, the sliding errors and the relative strut length errors are important factors affecting the machine tool accuracy.

Acknowledgement

The financial support received for this work from the Industrial Technology Research Institute of Taiwan is gratefully acknowledged.

References

1. K. M. Lee, D. Dharman and K. Shah, "Kinematic analysis of a three-degrees-freedom in parallel actuated manipulator", IEEE Transactions on Robotics and Automation, pp. 345–360, October 1988.
2. G. Lebret, K. Liu and F. L. Lewis, "Dynamic analysis and control of a Stewart platform manipulator", Journal of Robotic systems 10(2), pp. 629–655, 1993.
3. R. Nair and J. H. Maddocks, "On the forward kinematic of parallel manipulators", International Journal of Robotics Research, 13(2), pp. 171–188, 1994.
4. G. R. Pennock and D. J. Kassner, "The workspace of a general geometry for 3-DOF platform manipulator", ASME Journal of Mechanical Design, 115, pp. 269–276, 1993.
5. R. P. Podhorodeski and K. H. Pittens, "A class of parallel manipulators based on kinematically simple branches", ASME Journal of Mechanical Design, 116, pp. 908–914, 1994.
6. D. Kim, W. Chung and Y. Yonm, "Singularity analysis of 6-DOF manipulators with the analytical representation of the determinent", Proceedings IEEE International Conference on Robotics and Automation, pp. 889–894, 1999.
7. C. Park, "Computational aspect of manipulators via product of exponential formula for robot kinematics", IEEE Transactions on Automatic Control, 39(9), pp. 643–647, 1994.
8. G. Yang, M. Chen, W. K. Lim and S. H. Yeo, "Design and kinematic analysis of parallel robots", Proceedings IEEE International Conference on Robotics and Automation, pp. 2501–2506, May 1999.
9. J. Wang and O. Masory, "On the accuracy of a Stewart platform–Part I The effect of manufacturing tolerances", Proceedings IEEE International Conference on Robotics and Automation, 1, pp. 114–120, 1993.
10. T. Ropponen and T. Arai, "Accuracy analysis of a modified Stewart platform manipulator", Proceedings IEEE International Conference on Robotics and Automation, pp. 521–525, 1995.
11. A. J. Patel and K. F. Ehmann, "Volumetric error analysis of a modified Stewart platform-based machine tool", Annals CIRP, 46(1), pp. 287–290, 1997.